CHALMERS

Evaluation of manganese-silica oxides as oxygen carrier for Chemical-Looping Combustion at high temperatures

Master of Science Thesis

DANIEL CALVO CAMPOS

Department of Energy and Environment

Division of Energy Technology

CHALMERS UNIVERSITY OF TECHNOLOGY

Göteborg, Sweden, 2013

Contents

1. **Introduction**

Nowadays, it is not a novelty to state that a new energy era is coming. Oil reserves are predicted to be depleted in decades. Thus, an important challenge is headed to scientist community to find alternative sustainable energy sources. Many factors, such as economic viability, environmental impact or transportability need to be taken into consideration in research. Until feasible and completely sustainable new sources of energy would have been developed, several strategies must be applied to reduce serious negative effects on the earth caused by combustion of fossil fuels. Fossil fuel combustion emits thousands of tons of CO_2 every year and will still be the main energy source in foreseeable decades. Under such circumstances, CO_2 capture and storage is one of the most important strategies demanding to be carried out.

1.1. **Global warming and the greenhouse effect**

Global warming is a phenomenon that the average global temperature increases due to anthropogenic activities. The top ten warmest years since global temperature has been recorded all occur during 1997-2008 [1]. Further, it is predicted that the rising of average temperature will accelerate in 21th century. Although irreversible changes have been done to earth's ecosystem, worse situations can be avoided if proper actions are taken, for instance, mitigation and adaptation strategies. [2] Mitigation against climate change aim at decreasing anthropogenic emission of greenhouse gases, thus to suppress the rate of long-term environmental deterioration. To already existing climate change, adaptation strategy which acts to reduce potential damages caused by global warming is important. Mitigation and adaptation are considered as a medium-term solution, and technologies focusing on removing greenhouse gas emissions can play a significant role against global warming. Developing renewable and sustainable energy sources is another big part in mitigation strategy.

Greenhouse effect is the main reason for global warming. Greenhouse effect is a process where thermal radiation from earth is absorbed, and then re-radiated in all directions by atmospheric greenhouse gases. Since a part of this re-radiation is back towards earth, energy is transferred to the lower atmosphere and earth surface in form of heat. As a result, the average temperature on earth is higher than it would be if no greenhouse gases exist in the atmosphere. [3]With the increasing concentration of greenhouse gases (GHG) in atmosphere, the global warming effect is more and more severe in the past decades. Primary GHG are water vapor, carbon dioxide, CH_4, nitrous oxide and ozone [4]. Among them, CO_2 has the greatest greenhouse effect. The emitted CO_2 has the highest radioactive forcing and a lifetime over hundreds of years. What

worse is that CO_2 concentration in atmosphere keeps increasing since industry revolution age. The level of CO_2 has far beyond what ecosystem can balance by natural processes. In preindustrial era, CO_2 concentration was 280ppm. Nowadays, it is approximately 390 ppm in the atmosphere [5]. Burning of fossil fuels and deforestation are the main anthropogenic acts responsible for this rise. According to U.S. EPA (Environmental Protection Agency), the major GHG contribution to end-user sector is fossil fuel combustion industry and transportation [6]. So, reducing of CO_2 emissions from fossil fuel combustion is crucial.

1.2.   Combustion technology with CO_2 capture

To depress the amount of CO_2 emitted into atmosphere meanwhile still utilize fossil fuels as an energy source, CO_2 capture and storage (CCS) is proposed. In CCS process, CO_2 is first separated from other gases, then liquefied to facilitate transportation and stored. The first step in CCS, i.e. capture, can be practical at various industrial carbon dioxide producing sites. Condensed CO_2 can be stored in geological resources, for instance under the sea and in depleted oil fields. The captured CO_2 can also be used in other industrial processes, which is then another concept rather than CCS.

Considering CO_2 capturing, three technologies have been often discussed. They are: post-combustion, pre-combustion and oxy-fuel combustion. Though post-combustion and pre-combustion have been estimated economically feasible under specific conditions, neither of them have reached industrial level yet. On the other hand, oxy-fuel combustion is still under research phase. [7][8]

Post-combustion: the concept of this technology is to separate CO_2 from combustion exhaust gases. Calcium oxide looping [9] and chemical absorption by amines (e.g.: monoethanolamine (MEA), methyldiethanolamine (MDEA) or ammonia-base solutions) [10] are two widely studied processes for CO_2 separation. Other methods, such as physic adsorption, cryogenic distillation or membranes are also under development.

Pre-combustion: in pre-combustion technology, primary fuel mixed with steam and air (or oxygen) is processed in a reactor to produce carbon monoxide and hydrogen (syngas). In a second reactor (shifting reactor), CO reacts with steam producing H_2 and CO_2. In the last step, CO_2 is separated from hydrogen which is used in CO_2 free combustion. [11]

Oxy-fuel combustion: in this technology, O_2 is separated from air and mixed with CO_2 which is produced from combustion. Fossil fuels are burnt in O_2/CO_2 mixture instead of pure O_2 to avoid excessive heat release. The exhaust stream then consists of only steam and CO_2. CO_2 is typically about 90% and recirculated to the combustor mixing with O_2 after steam condensation. In oxy-fuel combustion, formation of NO_x is reduced by around 70-80% compared with normal combustion. On the other hand, SO_x may cause problems, such as high-temperature corrosion

on boilers' surface. So SO_x needs to be removed from the recycle CO_2 stream. [12] Oxy-fuel combustion technique is chiefly used in new-generation power plants with water-vapor cycles or gas turbines.

From economy point of view, a previous research estimated that applying CO_2 capture to combustion would involve an increase of electricity generation about 0,01-0,05 U.S.\$ per kWh, depending on the kind of fuel, the specific technology, the location and the national circumstances [13]. Since many variables affect electricity price (e.g. fluctuant evolution of fossil fuel price, costs added by CO_2 capture, price reductions due to better CH_4 extraction, etc.) a comprehensive economy study may be of great interest. Nevertheless, it is expected that building new power plants including CO_2 capture technologies would obtain higher efficiency of electricity generation and lower costs compared to adapting old ones.
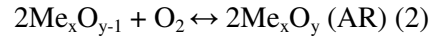
1.3.   Chemical Looping Combustion (CLC)

A promising innovative technology, Chemical Looping Combustion (CLC) is under development. With this technology, the O_2 in combustion air is partly removed by oxidation of a transition metal oxide (an oxygen carrier) which is reduced by fuel afterwards. In this way, the combustion needed O_2 is transferred to fuels without the necessary of gas separation.

Chemical Looping Combustion is not a new concept. In 1954, Gilliland patented "Production of industrial gas comprising carbon monoxide and hydrogen". This patent described a method using a metal as an oxygen carrier, which was oxidized in air, and reacts with hydrocarbon in fluidizing conditions to produce syngas. This can be regarded as the first on paper record of CLC concept. Between 1950 and 1954, Gilliland, together with Lewis, published an article titled "Production of pure carbon dioxide" using the same method. Richter and Knoche proposed that CLC process can be beneficial in combustion with the advantage of increased combustion efficiency. [14] Not until a thermodynamic study carried out by Ishida did the mentioned above process start to be identified as it is currently known as CLC. Seven years later, Ishida proposed CLC as a technique to capture CO_2. [15] In the last decade, academic publications related to CLC have exponentially increased. And lab scale CLC unit has scaled up to 1 MW_{th} in Damstadt, Germany.

A Chemical Looping Combustion unit consists of two fluidized bed reactors (an air reactor and a fuel reactor) where a metal oxide is used as an oxygen carrier to transfer O_2 from the air reactor (AR) to the fuel reactor (FR). The oxygen carrier is oxidized in the AR, and then circulated to the FR where it is reduced giving O_2 to fuel. The reduced oxygen carrier then returns to the AR and a new cycle continues. Main reactions that take place in a CLC cycle are:

$$C_nH_{2m} + (2n+m)Me_xO_y \leftrightarrow nCO_2 + mH_2O + (2n+m)Me_xO_{y-1} \quad (FR) \qquad (1)$$

$$2Me_xO_{y-1} + O_2 \leftrightarrow 2Me_xO_y \text{ (AR) (2)}$$

As seen from eq.(1), the outlet stream from FR is a mixture of steam and CO_2 if fully conversion is obtained. After steam condensation, pure CO_2 is ready for compression, transportation and storage.

By adding eq.(1) and eq.(2), one can find that the heat generated by CLC is the same as by normal combustion. So there is no energy loss involved in CLC. [16] Moreover, energy compensation for gas separation is overcome since CO_2 is inherently separated in CLC. Another advantage of CLC is that the generation of NO_x is avoided as no N_2 is presented in the fuel reactor.
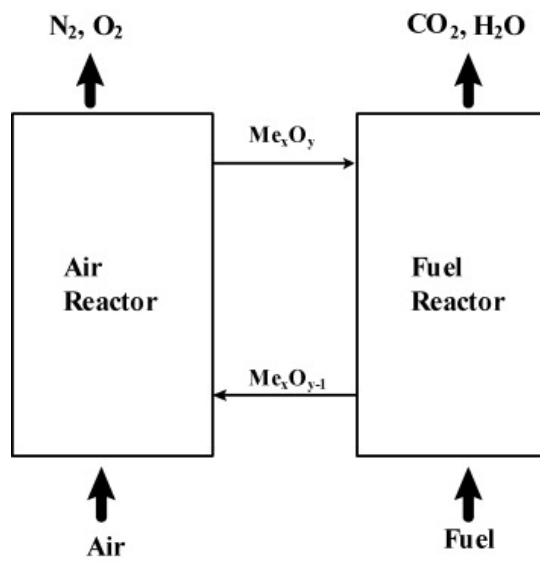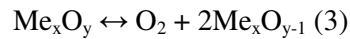

Fig.1 - Schematic representation of the CLC process.

1.4.   Chemical looping with oxygen uncoupling

To combust solid fuels, chemical looping with oxygen uncoupling (CLOU) represents an advantage compared to CLC. In CLOU process, oxygen carrier in the FR releases gaseous oxygen through decomposition according to reaction (3).

$$Me_xO_y \leftrightarrow O_2 + 2Me_xO_{y-1} \text{ (3)}$$

Thus, gas-phase oxygen reacts with the fuel according to reaction (4).

$$C + O_2 \leftrightarrow CO_2 \text{ (4)}$$

Since the contact between gas and solid molecules are more efficient than the solid-solid contact, CLOU is more favorable for solid fuel combustion than CLC. And by applying CLOU, slow gasification step can be escaped. [17][18] But from thermodynamic point of view, CLOU puts

restrictions on oxygen carriers. Not all oxygen carriers have appropriate thermodynamics properties to release O_2 in the FR. Some metal oxides systems, such as CuO/Cu_2O, Mn_2O_3/Mn_3O_4 and Co_3O_4/CoO have been proved having suitable equilibrium oxygen partial pressures at temperature 800-1200°C, thus having the ability to release gaseous oxygen in FR under combustion conditions. [19]
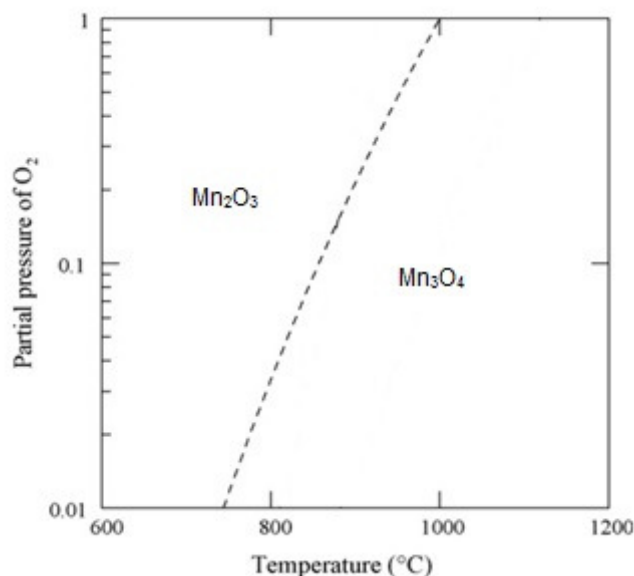

Fig.2 – The equilibrium O_2 partial pressure of Mn_2O_3/Mn_3O_4 system as a function of temperature.

Equilibrium oxygen partial pressure as a function of temperature for Mn_2O_3/Mn_3O_4 system is presented in Fig.2. At lower temperature or higher oxygen partial pressure, Mn_2O_3 is the stable phase. At higher temperature or lower oxygen partial pressure conditions, decomposition of Mn_2O_3 to Mn_3O_4 occurs with the release of gaseous oxygen. Assuming that AR has a temperature of 811°C and the outlet concentration is 5%, Mn_2O_3 is the phase presenting in solid stream. Whereas, in FR where O_2 concentration is 0% (assuming a same temperature as in AR), Mn_3O_4 is the stable phase suggested by Fig.2. So when the oxidized oxygen carrier is circulated from the AR to the FR, it releases gaseous O_2 due to Mn_2O_3 to Mn_3O_4 phase transition. This released O_2 can be directly used for fuel combustion. After reduction, oxygen carrier particles will be oxidized in the air reactor again.
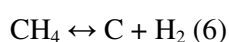
1.5.   Oxygen carriers

For CLC to be application feasible, some properties are demanded on oxygen carriers. These are: sufficient reaction rate of oxidation and reduction, ability to perform high conversion of fuel to CO_2 and H_2O, good fluidizing properties, resistance against attrition and fragmentation, life time corresponding to the price and friendliness towards environment. [20] Many materials have

been studied, and the potential candidates are: Ni-based, Cu-based, Mn-based and Fe-based oxides. [21]

Fluidizing ability is a key factor that needs to be taken into consideration when an oxygen carrier is evaluated. It is deemed particles have good fluidization property if no agglomeration or channel formation is observed under experimental period. Numerous factors may affect fluidization property of particles, such as size and shape of particles, size distribution of solids, vessel geometry, gas inlet arrangement, type of solid, degree of moisture and so on. [22]Reichold et al. described that the tendency to defluidize increases with increased temperature, and becomes less likely with increasing gas velocity and mean particle diameter of the bed material. [23]

Some support materials, aiming to improve oxygen carriers' resistant towards attrition, have been investigated (e.g. Al_2O_3, ZrO_2, TiO_2, SiO_2, MgO). In some cases, they may react with the active phase of an oxygen carrier forming new compounds which might affect the original properties of the oxygen carrier.

Another issue is carbon formation and its mechanism can be generally described by eq.(5)(Boudouard reaction) and eq.(6). Carbon formation has been noticed when operating some oxygen carriers. Metallic Ni is a catalyst for both eq.(5) and eq.(6). So if NiO oxygen carrier was further reduced and exposed to fuel rich condition, carbon formation can easily occur. Deposited carbon has been reported existing at the exit of FR reactor when operating some Mn-based particles. [24]

$$2CO \leftrightarrow CO_2 + C \ (5)$$

$$CH_4 \leftrightarrow C + H_2 \ (6)$$

1.5.1. Mn oxides oxygen carriers

Manganese oxide is characterized by its low price, abundance in natural reserves and promising performances reported as a CLOU material, which makes it a potential applicable OC.

The oxidation and reduction behavior of manganese oxides has been studied by E.R. Stobbe et al.[25]It was found that both MnO_2 and Mn_2O_3 had the ability to convert CH_4 at temperature above 800°C.When re-oxidize the reduced sample by 5% O_2(compensated by Ar) at 800°C, Mn_3O_4 was the identified phase instead of Mn_2O_3, even though Mn_2O_3 was the thermodynamic stable phase.[25] The suggested reason in the literature for this contradictive result was that the oxidation condition (5% O_2 and 800°C or temperature above) was too close to the Mn_2O_3/Mn_3O_4 equilibrium condition. So the driving force for Mn_3O_4 oxidation to Mn_2O_3 was

too low. Thus, to oxidize Mn_3O_4 to Mn_2O_3, either higher oxygen partial pressure or lower operation temperature was recommended.

The problem that Mn_3O_4 cannot be oxidized by lower oxygen partial pressure at high temperature is a barrier for Mn_2O_3 being applied in CLC as oxygen carrier. Except decreasing oxidation temperature or increasing oxygen partial pressure, another option to avoid the Mn_3O_4 oxidation difficulty is to combine Mn with other element forming combined oxides. Forming combined oxides could be useful to alter the thermodynamic properties of manganese oxides, thus allowing the oxidation occurring under the described situation. Combined manganese iron oxides $((Mn_{0.8},Fe_{0.2})_xO_y)$ was examined as oxygen carrier and presented promising results in a batch reactor system. These oxygen carriers showed CLOU property at 850ºC with fast releasing rate, comparable to CuO-Cu_2O system, and complete conversion of CH_4. [26] Shulman et al. examined a combined manganese iron oxide with a composition of 80 wt%Mn_3O_4 and 20 wt%Fe_2O_3. The oxygen carrier's reactivity was observed increasing with conducted CH_4 cycles in a 41 cycles test. [27]

Magnesium oxides with addition of calcium hydroxide have been mixed with manganese oxides as well. Some of these materials showed very high reactivity towards CH_4 and no carbon formation was detected. The addition of calcium hydroxide facilitates oxygen release and combustion of CH_4. [28]

Another idea to produce combined manganese oxygen carrier is mixing Si with Mn. By adding Si into manganese oxides, different manganese silicates are formed depending on the actual composition and synthesis temperature. Fig.3 is a phase diagram of Mn-Si-O system in air.[29] As can be seen in the figure, manganese silicates can transform to a lower Mn valence phase at higher temperature, together with releasing of oxygen. This means that Mn-Si-O materials have CLOU property theoretically. And examination of Mn-Si-O oxygen carriers is of great interest.
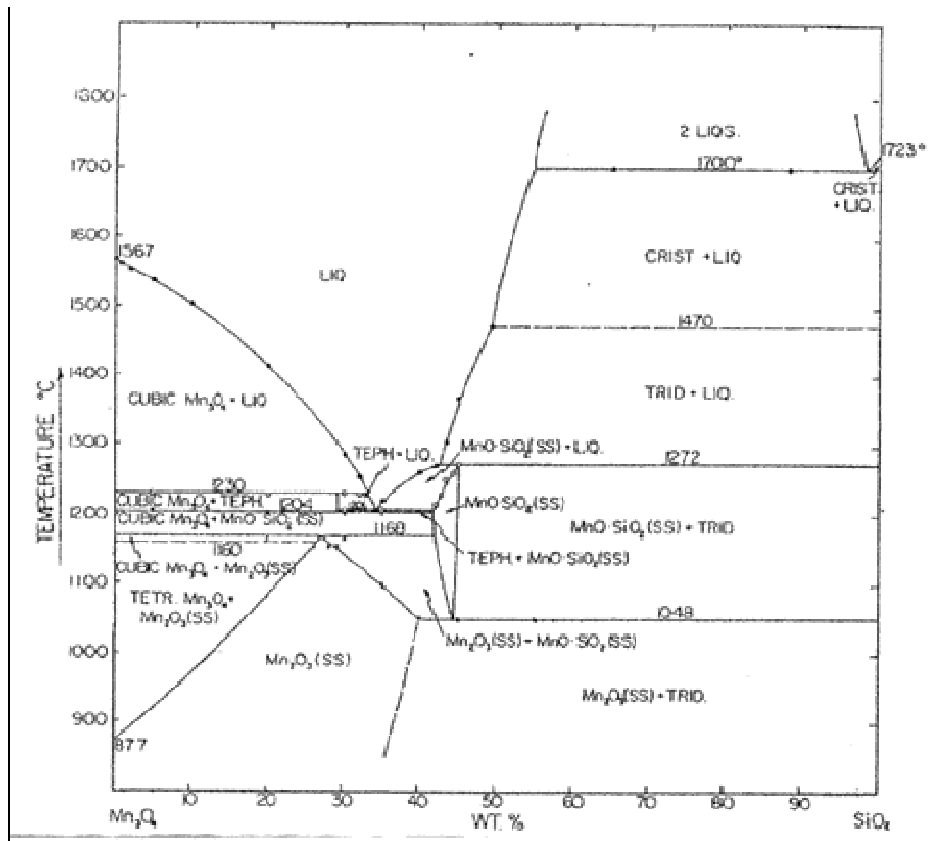
Fig.3 – Phase diagram of Mn-Si-O system in air [29]

An overview of combined manganese oxides that have been studied for CLOU application can be found elsewhere in literature. [30]

1.6. Objective

The aim of this project is to evaluate synthetic manganese silicate oxygen carriers for CLC and CLOU. In this work, 5 oxygen carrier materials with different Mn/Si ratio were manufactured by spray-drying and examined with respect to CLOU behaviour and CH_4 conversion at temperature 900ºC-1100ºC in a batch fluidized bed reactor system.

2. Experimental

2.1. Experimental setup

Oxygen carrier's reactivity test was performed in a batch fluidized bed system. As shown by Fig.4, the quartz reactor, which was 870 mm long and 22 mm in inner diameter, was enclosed in an electrical oven. In the quartz reactor, oxygen carrier was placed on a porous plate which was situated 370 mm from the bottom of the reactor. Temperature was measured 5 mm under and 10 mm above the porous plate by thermocouples enclosed in quartz shells. To examine fluidizing conditions, Honeywell pressure transducers with a frequency of 20 Hz were used to measure pressure drop over the bed.
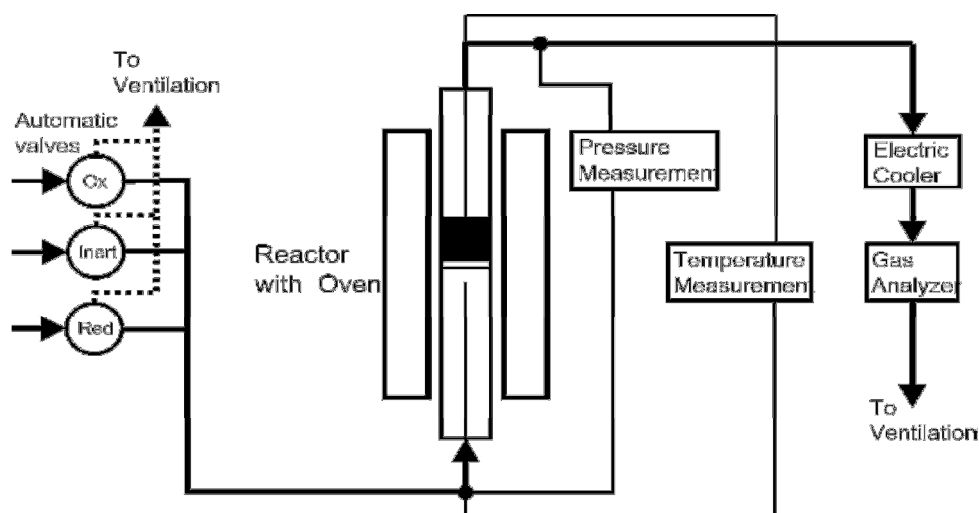

Fig.4 – Schematic demonstration of batch fluidized bed system.

Gas mixture of pure gas was introduced from the bottom of the reactor, reacted with oxygen carrier and left the reactor from the top. Outlet gas was first cooled by an electric cooler where the steam was condensed. Then the dry gas stream was sent to a gas analyser (Rosemount NGA-2000) where the volume fractions of CO, CH_4, CO_2 and O_2 together with a total volumetric flow were determined. Flue gases were driven to ventilation eventually.

2.2.   Manganese silicate particles in this study

Oxygen carriers investigated in this work were manufactured by spray drying. Detail information about spray-drying process was presented elsewhere in literature. [31] After spray-drying, produced particles were calcined at 1050ºC for 4 hours. Particles with diameter 125-180μm were sieved for reactivity test. In this project, the amount of Mn_2O_3 in raw material varied from 98 wt% to 50 wt%. A summary of raw material composition for spray-drying can be found in Table 1.

Table 1. Summary of raw material composition in spray-drying recipe.

Oxygen carrier	Composition	
	wt%Mn_2O_3	wt%SiO_2
M1	98	2
M2	94	6
M3	90	10
M4	50	50
M5	70	30

2.3.   Reactivity test of manganese silicate oxygen carrier

Evaluation of manganese silicate particles was divided into 3 parts:

o *Part 1:* Examine materials' CLOU property, reactivity towards syngas (50% CO and 50% H_2) and CH_4 at temperature 900ºC to 1100ºC after oxidation by 5% O_2.

o *Aim 2:* Examine oxygen carriers' CLOU behaviour under oxidation of 21%O_2.

o *Aim 3:* Examine stability of oxygen carrier's CLOU behaviour at a specific temperature by conducting multiple cycles after oxidation in 21%O_2.

In part 1, 15 grams of oxygen carrier was placed on the porous plate in the quartz reactor and heated to 900ºC under 5%O_2 (compensated by N_2). To activate oxygen carrier material, a syngas flow (450 mL/min) was injected into the reactor for 80s. After syngas reduction, particles were alternatively exposed to oxidation (5% O_2) and reduction (by CH_4 for 20s) environments, thus simulating the cyclic conditions of a CLC unit. A N_2 stream was injected for 60s before and after fuel inlet to avoid back-mixing of O_2 and fuel. In CH_4 cycles, CO_2 fraction was obtained, which can be directly related to CH_4 conversion, i.e. oxygen carrier's reactivity towards CH_4. Following two CH_4 cycles, two inert cycles were carried out, where N_2 (600 mL/min) was used to flush the reactor for 360s after particles being fully oxidized. This was to measure materials' CLOU property i.e. how much O_2 particles can release. Operation temperature was increased to next level during oxidation step after the two inert cycles were

finished. At each temperature, two CH_4 cycles and two inert cycles were performed as described above. Experimental temperature was set to 900ºC, 1000ºC, 1050ºC and 1100ºC.

Two oxygen carriers (M3 and M5), which presented better properties in part 1 test, were selected for part 2 test. Similar as performed in part 1, one syngas cycle and two inert cycles were conducted at each temperature, i.e. 900ºC, 950ºC, 1000 ºC, 1050ºC and 1100ºC, after particles were fully oxidized. Since M5 material showed better results, it was tested in an additional temperature range: 925ºC, 975ºC, 1025ºC and 1075ºC. In part 2, the oxidation condition was air which was different from part 1.

The stability of M5 oxygen carrier regarding CLOU property was evaluated in test Part 3. Experimental temperature was set to 1000ºC, where M5 material demonstrated highest reactivity observed from the first part of the work. In this part of test, M5 particles were firstly activated by conducting four syngas cycles (80s syngas injection in each cycle). Then, eight inert cycles (N_2, 360s flushing) were performed. After both syngas and N_2 cycles, air was used to oxidize the sample.

Fresh particles were used in all three parts of tests. Gas composition and flows were summarized in the table below.

Table 2. Summary of the gas flows in each cycle. [1]Only one fuel is used in each cycle.

		Cycle		
		Oxidation	**Inert**	**Reduction**
AIM 1	**Air (21% O_2, 79% N_2)**	216,35 ml/min	-	-
	Nitrogen	683,65 ml/min	600 ml/min	-
	CH_4[1]	-	-	450 ml/min
	Syngas (50% H_2, 50% CO)[1]	-	-	450 ml/min
AIM 2&3	**Air (21% O_2, 79% N_2)**	600,55 ml/min	-	-
	Nitrogen	-	600 ml/min	-
	Syngas (50% H_2, 50% CO)	-	-	450 ml/min

Crystalline phases of M5 particles were identified by X-ray powder diffraction. Fresh samples, samples oxidized by 5% O_2 air and syngas reduced sample were examined. The oxidized samples were obtained by exposing the fresh sample to an oxidizing flow (5%O_2 or 21%O_2, respectively) at 1000ºC for 45 minutes, and then cooled in the respective oxidizing flow as rapid as possible to room temperature. The reduced sample was achieved by running syngas through the reactor at 1000ºC for 15 minutes, ensuring the reduction of the whole sample, and cooled down to room temperature in syngas.

2.4.   Data Analysis

Gas yield (γ) is used to gauge the reactivity of an oxygen carrier towards a fuel. It is defined as the percentage of a product compound over the total amount of compounds in the outlet stream. In this study, gas yield is chosen as the CO_2 percentage in the outlet stream. With CH_4 or syngas as reducing gas, γ is expressed as follows:

$$\gamma = \frac{x_i}{\sum_{i=1}^{n} x_i} \quad (7)$$

where x_i is the fraction of component i (for CH_4 cycle i=CO, CO_2 and CH_4; for syngas cycle, i=CO and CO_2) in the dry outlet gas. CO_2 is used to calculate gamma as it is the most oxidized product. The gamma value ranges from 0 to 1, where 1 refers to complete conversion.

The degree of mass-based conversion, ω, is defined as the mass of the oxygen carrier divided by the mass when it is fully oxidized:

$$\omega = \frac{m}{m_{ox}} \quad (8)$$

Since m is not practical to be directly measured, it can be calculated as a time integral during a reduction period. When CH_4 was used as fuel, it can be obtained by equation 9:

$$\omega_i = \omega_{i-1} - \int_{t_0}^{t_1} \frac{\dot{n} M_0}{m_{ox}} \left(4 x_{CO_2} + 3 x_{CO} - x_{H_2}\right) dt \quad (9)$$

where $\dot{n}$ is the molar flux of the dry outlet stream and M_0 is the molar mass of oxygen. When syngas is the fuel, ω can be calculated as:

$$\omega_i = \omega_{i-1} - \int_{t_0}^{t_1} \frac{\dot{n} M_0}{m_{ox}} \left(2 x_{CO_2} + x_{CO} - x_{H_2}\right) dt \quad (10)$$

3. Results and discussion

3.1. Reactivity towards syngas

At the beginning of test part 1, one syngas cycle was performed at 900ºCafter sample particles were fully oxidized. This syngas cycle aimed to activate oxygen carrier particles and the gas conversion in the cycle was analyzed to present material's reactivity towards syngas.
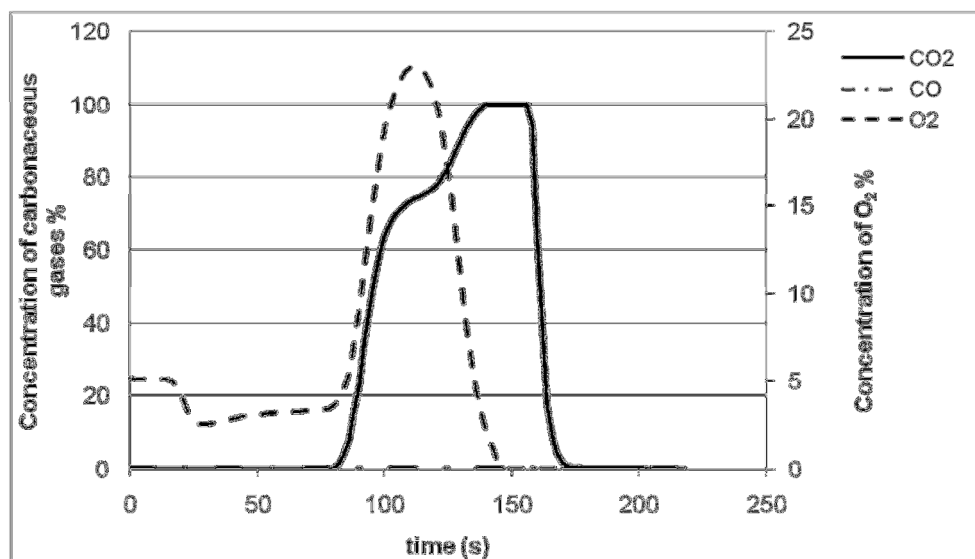

Fig.5 – Dry gas concentration profile of outlet stream in a syngas cycle performed on M3 sample.

Fig.5 is an example of dry gas concentration profile of a syngas cycle at 900ºC, where M3 material was chosen. At t=0 s, 5% O_2 was switched off and pure N_2 was inlet into the system for 60 s. The decreasing of O_2 concentration cannot be noticed until t= 20 s due to a delay of the measuring system. At t=80 s, syngas was injected into the reactor while N_2 was turned off. At this time, a rapid raising CO_2 concentration was detected suggesting that the inlet syngas was fast converted into CO_2 by M3 oxygen carrier. Reading from the figure, one can see that O_2 concentration increased considerably from 5% (oxidizing condition) till over 20% after syngas injection. Syngas conversion over manganese silicate oxides was highly possible an exothermal reaction suggested by measured increasing temperature. This could be a cause for the increased O_2 concentration. Referring to Fig.3, as surrounding temperature increased, the manganese silicate can decompose to a lower Mn valence manganese silicate, which released more O_2 compared with the case having a stable temperature. During calcination, oxygen carrier particles were heated and cooled down to room temperature in air. Under such a circumstance, some O_2 may be trapped in the particles due to solid shrinkage. These O_2 might be released during syngas reduction cycle as a result of particle expansion. Thus, these trapped O_2 could be the main reason for the observed huge amount of released O_2 as manganese silicate phase transition

is theoretically not able to provide such a quantity of O_2. Afterwards when oxygen concentration decreased till 0%, just CO_2 was detected. Gas yield of syngas was calculated and full conversion was obtained. For the other tested oxygen carriers, the O_2 concentration peak during syngas reduction cycle varied from 7% to 24%. But all materials achieved full conversion of syngas. Therefore, oxygen carriers' reactivity towards fuel was focused on CH_4 conversion.
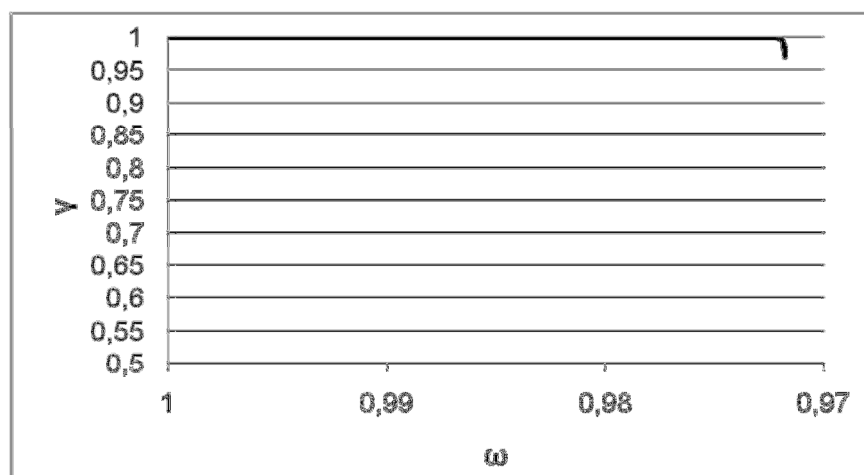

Fig.6 – Gas yield (γ) as a function of mass-based conversion (ω) for M3 carrier using syngas as fuel

3.2. Reactivity towards CH_4

CH_4 is the primary constituent of natural gas which may be an alternative fuel instead of coal in the future.

In part 1 test, two CH_4 cycles were executed at each temperature (900ºC, 1000ºC, 1050ºC and 1100ºC). Some information at high temperatures is missing due to de-fluidization problem of some samples. The dry gas concentration profile of the 2nd CH_4 cycle performed on sample M3 at 1000ºC is presented in Fig.7 for demonstration. At 30s<t<90s, all carbon gas concentrations were 0 since the reactor was purged by a nitrogen stream. During the fuel cycle (80s<t<100s), 93% of CH_4 was converted to CO_2, despite of a small amount of unreacted CH_4.
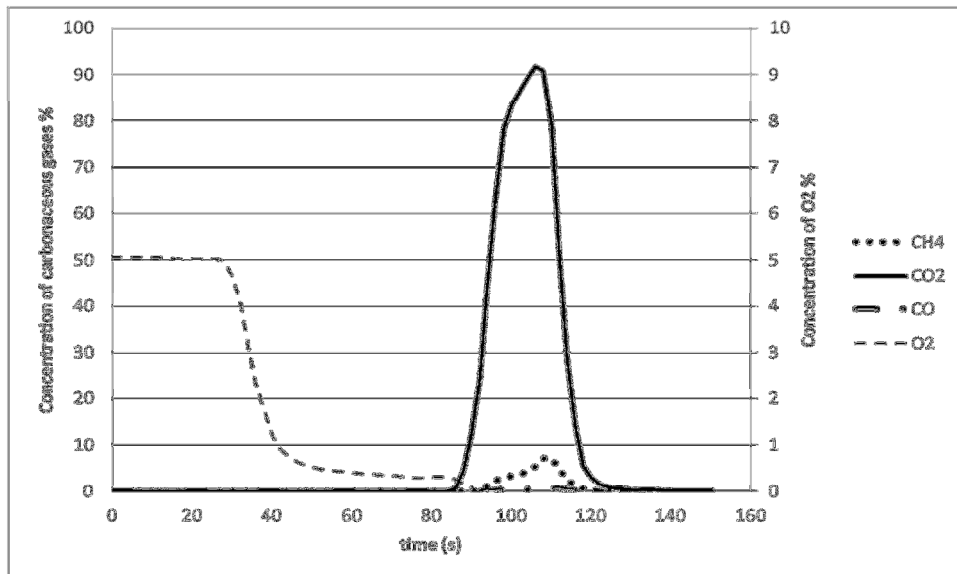
Fig.7 – Dry gas concentration profile of outlet stream for the 2nd CH₄ cycle at 1000ºC performed on M3 sample.

Fig.8a shows the CH$_4$ yield (γ) as a function of the solid conversion (ω) for M3 carrier investigated at four different temperatures. Black colored lines present results obtained from the first CH$_4$ cycle and red colored lines are the situations for the second CH$_4$ cycle. As seen in the figure, M3 sample's reactivity was almost identical for the two CH$_4$ cycles performed at the same temperature. Generally, the gas conversion was high at higher experimental temperatures. In some cases (M1 or M2), particles performed forming channels or soft agglomerations at temperatures over 1050ºC, resulting in fluidization problems.
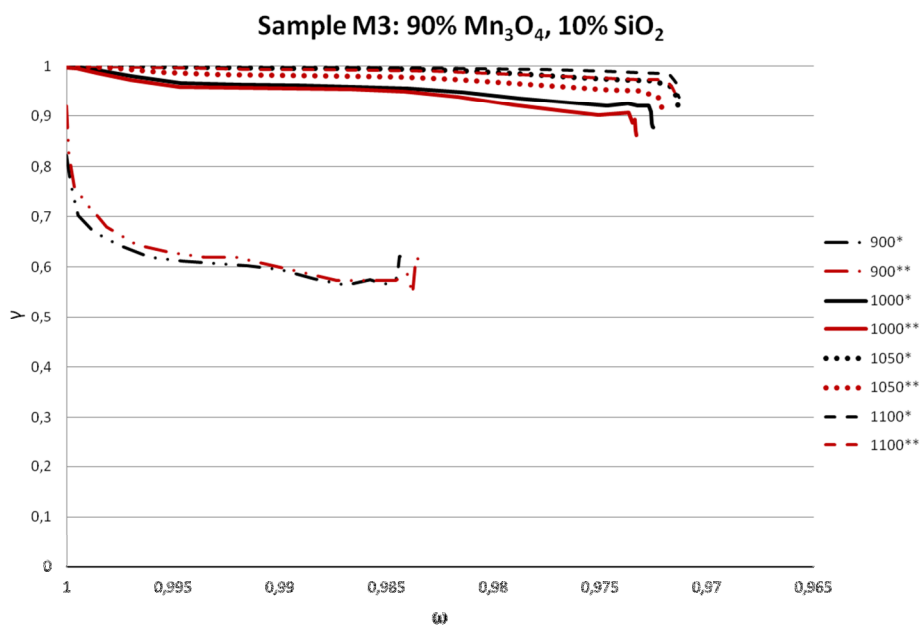

Fig.8a – Gas yield (γ) as a function of mass-based conversion (ω) for M3 carrier using CH$_4$ as fuel.

The γ-ω plots for M4 particles at different temperatures are presented in Fig.8b. Compared with M3 sample, see Fig.8a, M4 particles presented a different behavior. The reactivity of M4 materials increased with experimental temperature from 900ºC till 1000ºC. Further temperature increase resulted notably deactivation shown by the dotted lines and dashed lines in the figure below. Severe deactivation of material's reactivity towards CH_4 at higher temperature was only observed on M4 sample.
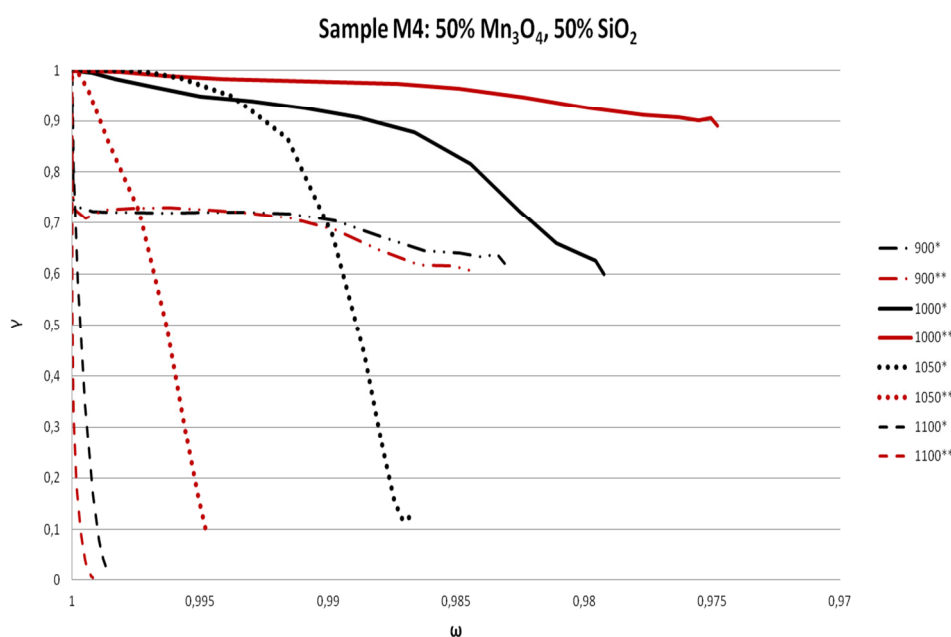

Fig.8b – CO_2 yield (γ) as a function of mass-based conversion (ω) for M4 carrier using CH_4 as fuel.

Fig.9 summarizes the CH_4 conversion at four experimental temperatures for all tested manganese silicate oxygen carriers. Each point refers to an average CH_4 conversion at a certain temperature from where a comparison among the examined samples can be accomplished. At 900ºC, gas yield ranged from 70 to 80% for all the particles, except for M1. Although M1 possessed the highest composition of manganese oxide, it presented the lowest reactivity towards the fuel at temperature range 900ºC to 1000ºC. It seems that samples with higher Si content had better reactivity at temperature 900ºC to 1000ºC. In this temperature range, manganese silicate oxygen carriers' reactivity increased obviously with experimental temperature. Sample M2, M3 and M5 retained full CH_4 conversion under high temperature conditions, i.e. 1050ºC and 1100ºC. On the other hand, M1 sample suffered defluidization at 1100ºC and M4 material's reactivity sharply decreased when temperature increased from 1000ºC to 1100ºC.

Compared with pure manganese oxides, addition of Si indeed improved oxygen carriers' properties. [21] During experimental process, no difficulty in oxidizing Mn-Si oxygen carrier at

temperature above 900ºC was observed. Material M2, M3 and M5 even had the ability to fully convert CH_4 at 1100ºC without any defluidization problem, which is very promising. The amount of added SiO_2 needs to be appropriate. Sample M1 with 2 wt% SiO_2 in recipe encountered defluidization problem at higher temperature, and M4 particles with 50 wt% SiO_2 in raw materials had extremely low reactivity at higher temperature. Suggested amount of SiO_2 to combine with Mn_3O_4 is between 6 wt% to 30 wt%.

The different behavior of M4 material, i.e. low reactivity at higher temperature, compared with the other tested materials may be briefly explained as follows. Referring to Fig.3, M4 sample containing 50 wt% of SiO_2 lay on the right hand side of the Mn-Si-O phase diagram, while the rest of tested samples lay at the left hand side of the phase diagram. At higher temperature, M4 sample fall into $MnO•SiO_2$ solid solution area and MnO is the most reduced phase of Mn oxides. This might be the reason for the extremely low reactivity of M4 sample at temperature above 1050 ºC. For M1, M2, M3 and M5 samples, several other manganese oxide phases with lower Mn valences exit at higher temperature, which could facilitate further reduction of oxygen carriers. This might explain the behavior that these samples maintained high reactivity at higher temperature.
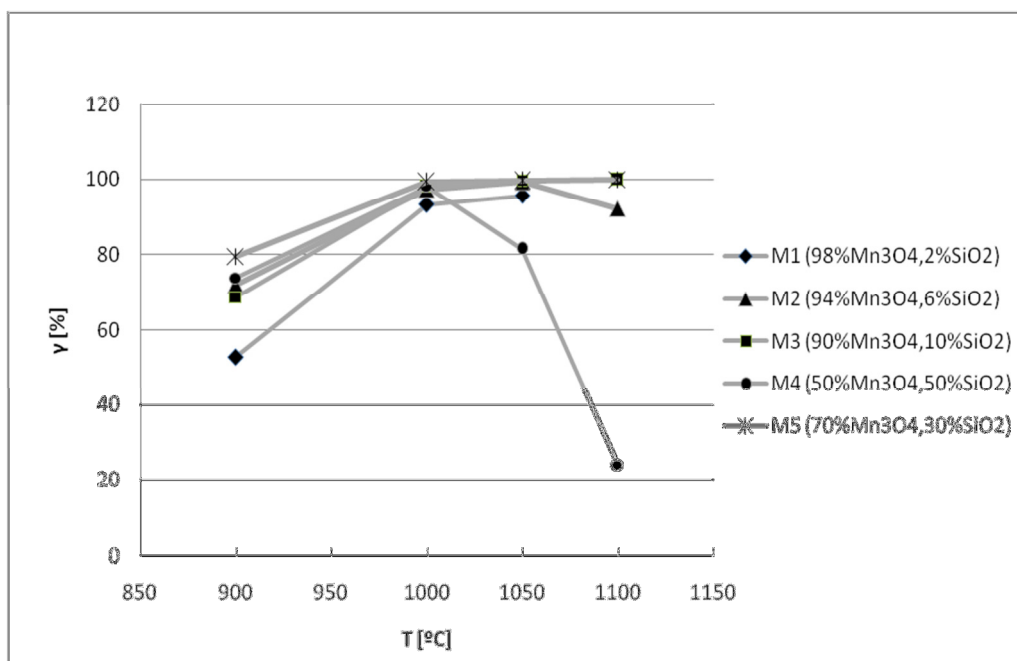

Fig.9 – Summary of CH_4 conversion at tested temperatures for five examined manganese silicate oxygen carriers.

3.3. CLOU property after oxidation by 5% O_2

Oxygen carriers' CLOU property was evaluated by operating inert cycles and measuring the O_2 concentration in the outlet stream. Since CLOU process is more favorable than CLC process, CLOU property of an oxygen carrier is an important factor to evaluate.

In test part 1, two inert cycles were conducted at temperature 900℃, 1000℃, 1050℃ and 1100℃ after CH_4 cycles. The O_2 concentration as a function of time for the second inert cycle at 1000℃ is plotted in Fig.10. At t=0 s, 5% O_2 used for particle oxidation was switched off and pure N_2 was sent into the system for 360 s. The O_2 concentration did not drop down until t=20 s. This was due to a system delay as described before. The O_2 concentration did not go to 0 immediately, but maintained at a certain level which was resulted from materials CLOU property.
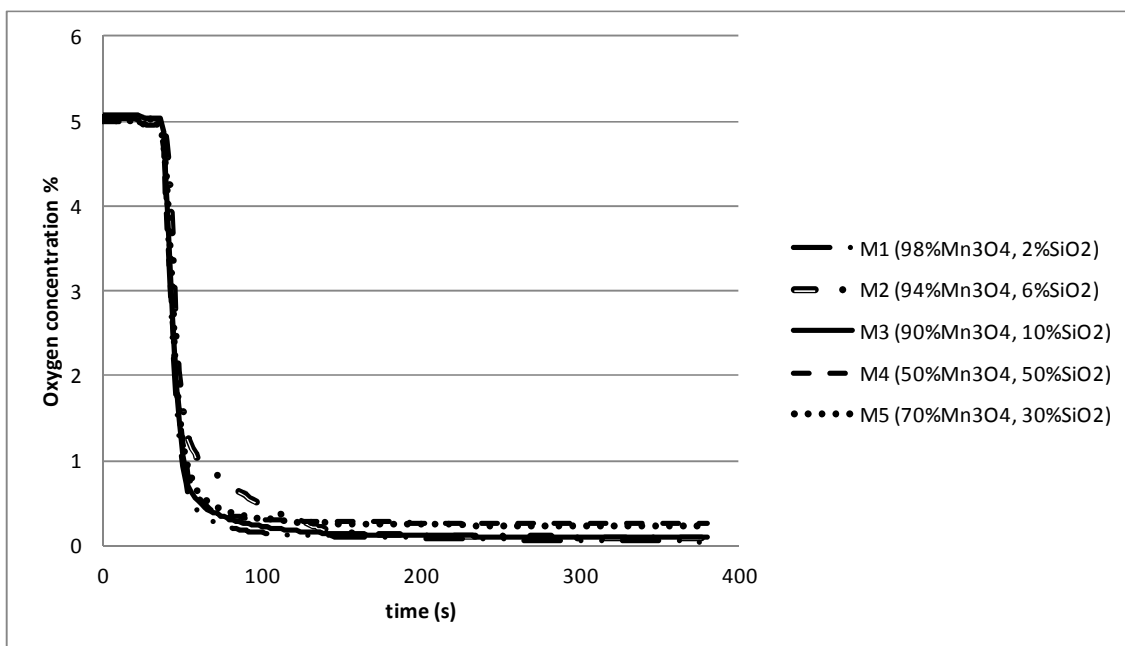

Fig.10 – The O_2 concentration profile of the 2nd inert cycle at 1000℃ for all tested materials.

Taking a closer look at the last 60 s of the O_2 concentration profile, presented in Fig.11, one can find that these manganese silicate oxygen carriers did not release too much O_2 at 1000℃. And material M4 and M5 which had higher SiO_2 contents released more O_2 than the other materials at 1000℃.
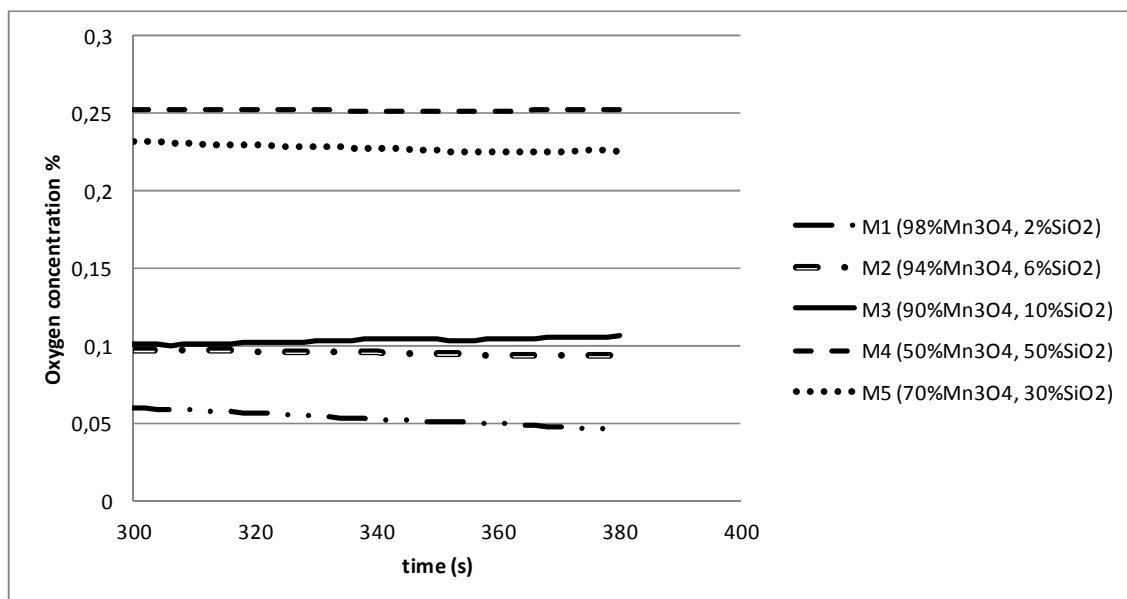
Fig.11 – The last 60 s of the O$_2$ concentration profile of the 2nd inert cycle at 1000ºC for all tested materials.

Fig.12 summarizes the concentration of released O$_2$ for all tested materials at four experimental temperatures. At each cycle, the O$_2$ concentration at t=360 s was selected to present material's CLOU property. The average value of two cycles at the same temperature was calculated to gauge material's CLOU property at this temperature. These calculated average value were plotted as a function as temperature and shown in Fig.12.

As shown in the following figure, manganese silicate oxygen carriers' CLOU property was suppressed at low temperature. With temperature increase, from 900ºC to 1000ºC, CLOU property of all tested materials was promoted. At 1050ºC, M1 material first encountered defluidization problem. Later, sample M2 and M5 had difficulty in fluidization at 1100ºC. Though M4 material did not have fluidization difficulty, its CLOU property greatly diminished when the experimental temperature increased above 1000ºC. On the other hand, the CLOU property of M3 particles which had 30 wt% Si content improved with increasing temperature. The released O$_2$ by M3 particles increased from 0.1% at 900ºC and reached a maximum of 0.7% at 1100ºC.
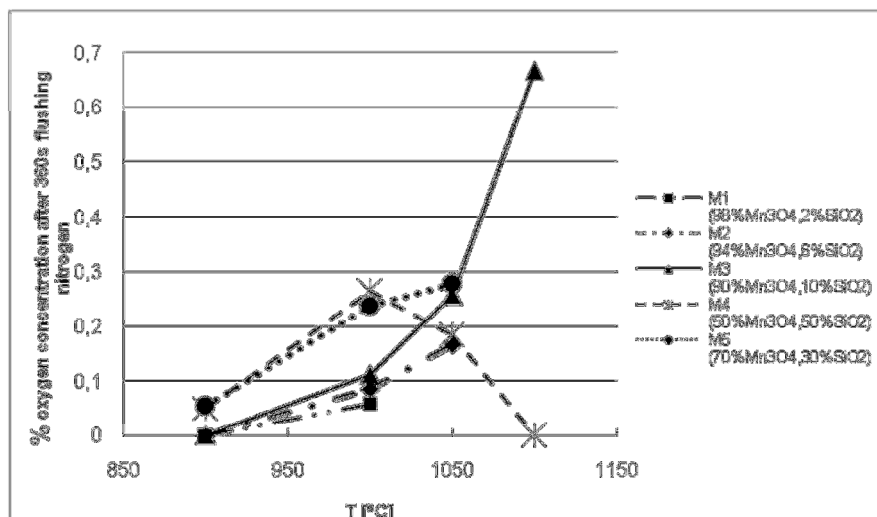
Fig.12 – The average concentration of released O₂ for tested oxygen carriers at four temperatures.

3.4. CLOU property after oxidation by air

Based on the results in section 3.3, two oxygen carriers M3 and M5, which presented better results at high temperatures, were chosen to investigate in part 2 test. In this part of test, particles were oxidized by air, i.e. 21% O_2, instead of 5% O_2. And experimental temperatures were set to 925ºC, 975ºC, 1025ºC and 1075ºC. Detailed experimental procedure can be found in section 2.3.
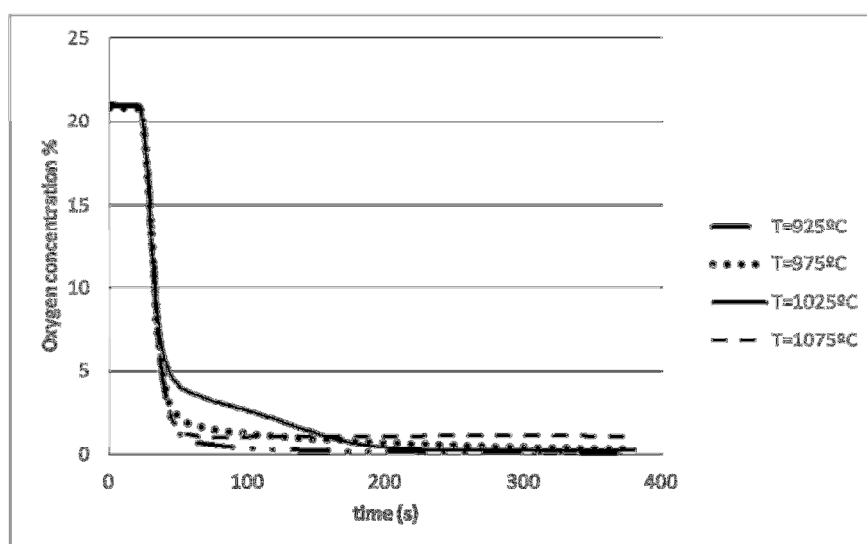

Fig.13 – The O₂ concentration profile of the 2nd inert cycle for M5 material. The oxidation gas was air for all cases.

In Fig.13, the O₂ concentration profile of inert cycles for M5 sample is presented. Oxygen carrier particles were fully oxidized by synthetic air before exposed to pure N₂ for 360s. The

drop of O_2 concentration was not observed until t= 20 s, though the N_2 flow was switched on at t=0 s. The O_2 concentration of the last 60 s is shown in Fig.14, where the influence of temperature is clearly seen. Generally, the M5 material's CLOU property improved with temperature. The maximum released O_2 was achieved at the highest experimental temperature 1075ºC, and almost no O_2 was released at 925ºC. At 1025ºC, M5 material's CLOU property was surprisingly low. Unfortunately, the reason for this is yet unknown and thus needs to be investigated in the future.
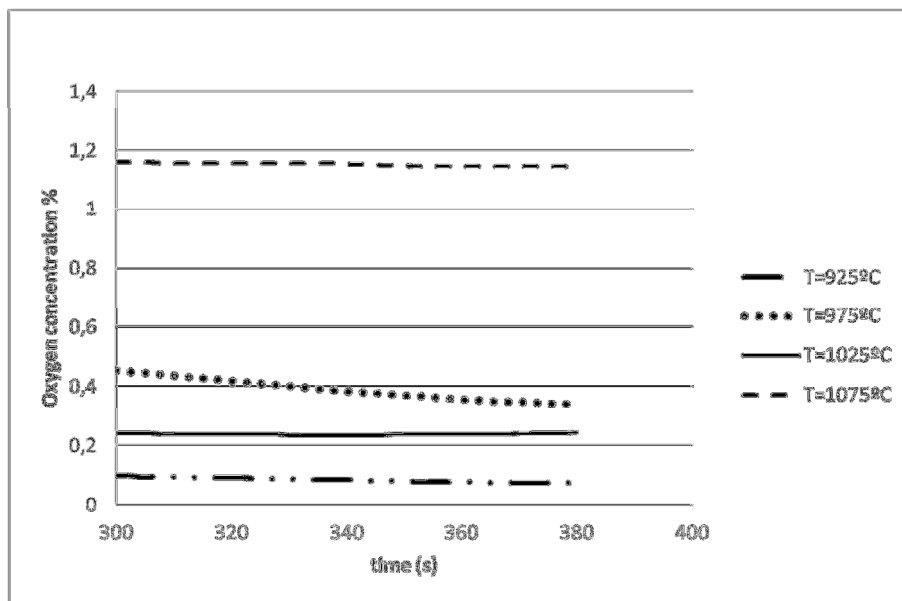

Fig.14 – The last 60 s of the O_2 concentration profile of the 2nd inert cycle for M5 materials.
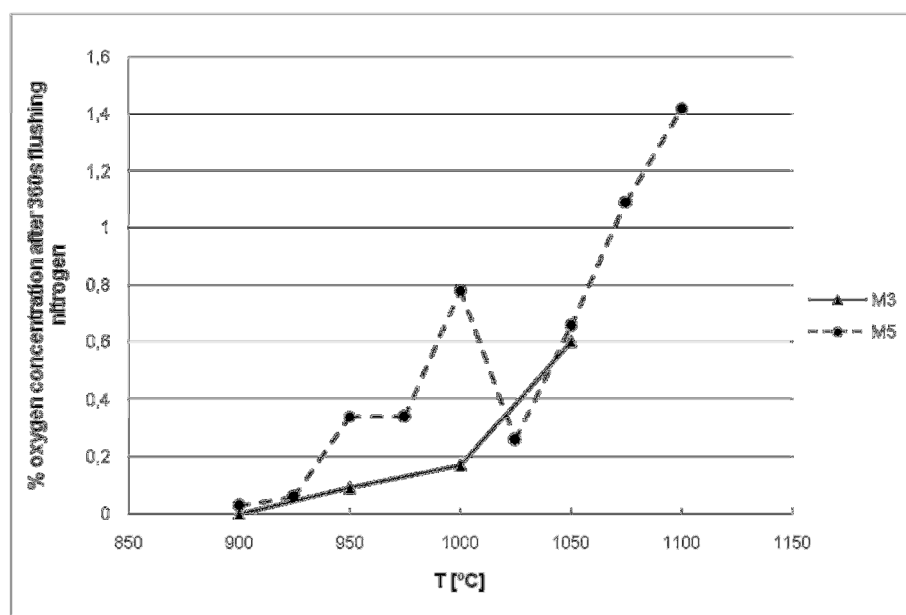

Fig.15 - The average released O_2 concentration for M3 and M5 carriers after oxidation by air.

Fig.15 summarizes the released oxygen concentrations at tested experimental temperatures of M3 and M5 particles after oxidation under air conditions. As described in section 3.3, the average value was calculated from O_2 concentration at t=360 s of which two inert cycles were performed at the temperature. From the figure, M3 material's CLOU property clearly showed an increasing trend with experimental temperature. At temperature range 1000ºC to 1050ºC, M3 materials' CLOU property was greatly promoted. While, the relationship between experimental temperature and CLOU property for sample M5 was not very straightforward. Positive effect of increasing temperature on material's CLOU property was observed from 900ºC to 1000ºC. Then CLOU property was sharply suppressed at 1025ºC. With further increasing of experimental temperature, M5 material's CLOU property was improved. The variability of trends may indicate more than one phase change occurred in temperature range 900ºC and 1100ºC for M5 particles.
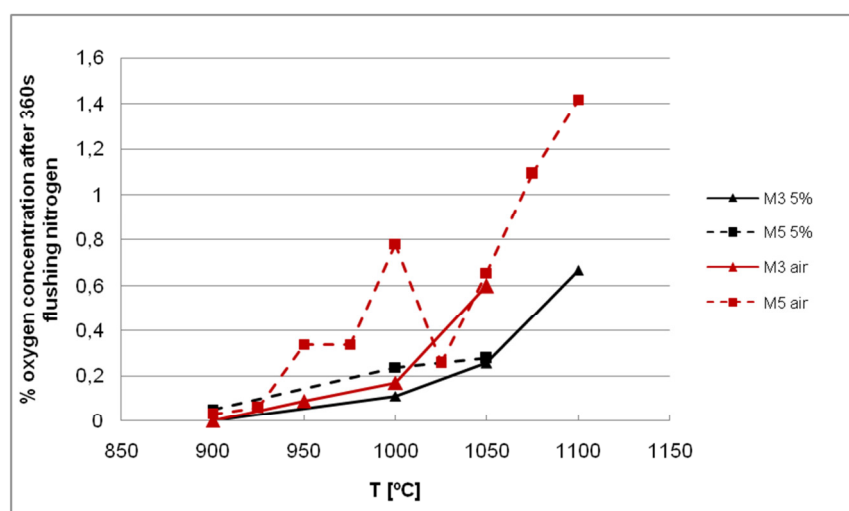

Fig.16 – Average released O_2 concentration for M3 and M5 carriers after oxidation by 5% and air

Fig.16 compares the average CLOU O_2 concentration in inert cycles after air and 5% O_2 oxidation for M3 and M5 particles. Red colored lines present the results obtained from air oxidation condition and black lines showed the 5% O_2 oxidation condition. Oxidation by a higher O_2 partial pressure stream apparently benefited materials' CLOU property. The positive effect of higher O_2 partial pressure was extremely important at higher temperature. Both M3 and M5 material released more than double amount of O_2 after oxidation by air than by 5% O_2 comparing the red dots and black ones at temperature 1050ºC and above. This effect is theoretically logical since equilibrium O_2 partial pressure for a certain phase transition is higher at higher temperatures. So, higher O_2 partial pressure is required to be able to oxidize oxygen carrier particles in some cases. With higher O_2 partial pressure, the particles may be more oxidized as the driving force is bigger compared with oxidation by a lower O_2 partial pressure stream.

3.5.   CLOU behavior in multiple cycles

The stability of a material's CLOU behavior is a key factor in CLOU. Oxygen carrier M5 was selected for the stability test which was described in part 3 test in section 2.3. At 1000ºC, a syngas cycle and an inert cycle were run alternatively for four times. Afterwards, eight inert cycles were executed.
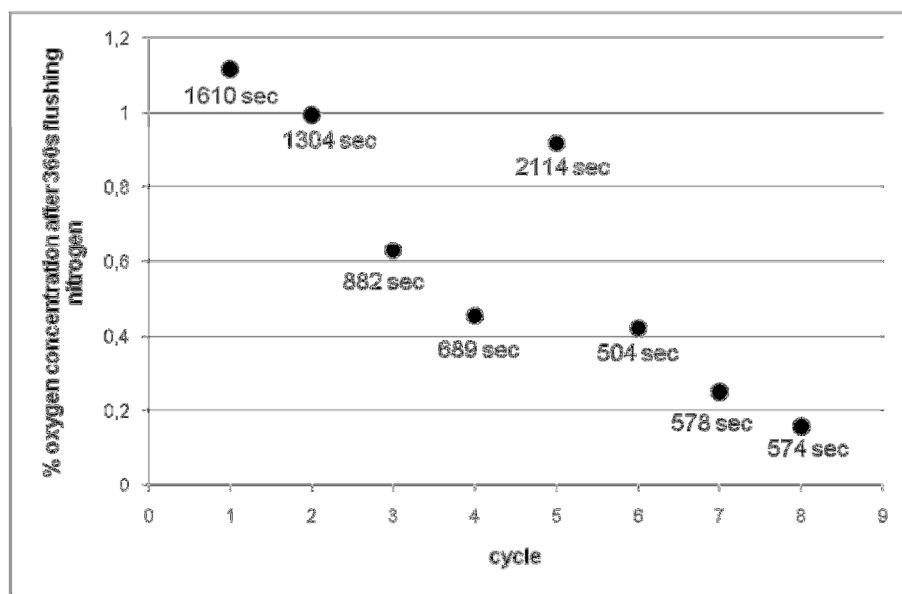

Fig.17 –Oxygen concentration released by M5 carrier at 1000ºC in multiple inert cycles.

Fig.17 presents the oxygen concentrations released by M5 carrier at the end of inert cycle where t=360 s. Particles were previously oxidized by 21% O_2 air. As seen from the figure, the CLOU property of M5 decreased obviously along the number of performed cycles. Time of oxidation, which was indicated below each experimental point, seems to be a factor influencing how much oxygen can be released in the following inert cycle. However, the deterioration of CLOU ability cannot be fully overcame by increasing oxidation time as implied by the last three cycles. Since experimental condition was thermodynamically sufficient to fully oxidize the particles, the decreasing of CLOU property with prolonged cycles may be caused by a low diffusion inside the particles.

3.6.   M5 phase analysis by XRD

Table 3 presents the XRD identified crystalline phases on M5 samples. Fresh sample was the particles before running any gas cycles. Oxidizing samples were the ones oxidized by the indicating gases at 1000ºC for 45 minutes, and then cooled in 5%O_2 or synthetic air, rapidly to room temperature. Reduced samples were obtained by reducing the sample by syngas for 15 min and fast cooled to room temperature in syngas flow.

Surprisingly, particles oxidized by 5% O_2 and reduced by syngas, column 2 and 3, had the same composition. This was theoretically impossible as the material converted syngas losing oxygen and being reduced. Since XRD scanning period was set to 15 min which was quite short at some point, there could be some information missing or hiding in the low intensity area in the result diffraction spectra. This is a factor needs to be taken into consideration.

Particles oxidized by air and then reduced by syngas presented a different phase compared with air oxidized sample, see column 4 and 5 in Table 3. In the reduced sample, tephroite Mn_2SiO_4 was identified instead of rhodonite $MnSiO_3$ in the oxidized sample. At 1000ºC, reaction between braunite and rhodonite forming tephroite seems to be the reaction contributing to syngas conversion for particles oxidized by air. This mechanism, where the different phases were actually detected in this work, was also suggested by Rydén et.al. [30]

Table 3 – Crystalline phases identified on M5 samples by XRD.

Oxygen carrier	M5 (70 wt% Mn_3O_4, 30 wt% SiO_2)				
Temperature	1000ºC				
Oxidizing/ Reducing gas	- (Fresh sample)	5%O_2, N_2 (oxidizing)	Syngas (reducing)	21%O_2, N_2 (oxidizing)	Syngas (reducing)
Phases identified	Braunite-1Q ($Mn_7O_8(SiO_4)$) Rhodonite ($MnSiO_3$)	Braunite-1Q ($Mn_7O_8(SiO_4)$) Rhodonite ($MnSiO_3$)	Braunite-1Q ($Mn_7O_8(SiO_4)$) Rhodonite ($MnSiO_3$)	Braunite-1Q ($Mn_7O_8(SiO_4)$) Rhodonite ($MnSiO_3$)	Braunite-1Q ($Mn_7O_8(SiO_4)$) Tephroite (Mn_2SiO_4)

In the case of M4 particles, a remarkable physical change took place. The bed material turned its color from initial brown to ash grey after test part 1. Seemingly, it may be caused by irreversible formation of silicate.

4. Conclusions

Five combined manganese silica samples with different Mn:Si ratio have been investigated in this work. The percentage of silica in raw materials increases from 2wt%, 6wt%, 10wt%, 30wt% to 50wt%. The following conclusions can be drawn:

- All manganese silicate oxygen carriers presented high reactivity towards syngas at 900ºC.

- Particles with a composition of silica between 6wt% and 30wt% showed great reactivity towards CH_4 at temperature 900ºC to 1000ºC. Furthermore, SiO_2 seems to improve materials' fluidization properties.

- Seemingly, materials CLOU property increased with silica content. Materials M4 containing 50 wt% SiO_2 and M5 with 30 wt% SiO_2 demonstrated better CLOU properties among the tested materials between 900ºC and 1050ºC.But at higher temperature 1100ºC, M3 material consisting of 10 wt% SiO_2 and 90 wt% Mn_3O_4 released about 0.7% O_2 which performed best.

- M3 material presented an increasing trend of releasing oxygen with increased temperature under experimental conditions.

- M5 proved to release the highest percentage of gaseous oxygen (1,4%O_2) at 1100ºC in N_2.

- The CLOU property of sample M5 decreased apparently when multiple inert cycles are carried out.

5. Acknowledgements

First of all, I would like to offer my special thanks to my supervisor Dazheng Jing for his useful critiques and constructive corrections, for his patience guidance and for his language corrections, even not being part of his task. I also would like to express my deep gratitude to Dr. Henrik Leion, for the opportunity to accomplish my master thesis with the CLC group at Chalmers University, and Professor Anders Lyngfelt, for leading the CLC group research. This work would not have been possible without them. My grateful thanks are extended to Golnar Azimi, Mehdi Armand, Peter Frohn, Martin Keller, Ali Hedayati and Nasim Mohammadpour for their help and kindness towards me. Finally, I would like to thank my parents for their support and encouragement throughout the whole process in my university stage.

References

[1]   NASA. *GISS Surface temperature Analysis. Global temperature Trends: 2008 Annual Summation.*

[2]   IPCC. *Synthesis Report Summary for Policymakers, Section 4: Adaptation and mitigation options*, in IPCC AR4 SYR 2007.

[3]   IPPC. *Summary for policymakers. Contribution of Working Group I to the Fourth Assessment Report of the IPPC*, 2007.

[4]   Kiehl J.T., Kevin E. Trenberth. *Earth's annual global mean energy budget.* Bulletin of the American Meteorological Society 78 (2): pp. 197–208.

[5]   ESRL. *Trends in carbon dioxide*. Esrl.noaa.gov. Retrieved 2011-09-11

[6]   U.S. EPA. *U.S. Greenhouse Gas Inventory - U.S. Greenhouse Gas Inventory Reports|Climate Change - Greenhouse Gas Emissions*. Epa.gov. 2006-06-28. Retrieved 2010-10-16.

[7]   The Global CSS Institute. The Global Status of CSS: 2011

[8]   The Global CSS Institute. *CO_2 Capture Technologies: Pre Combustion Capture*. January 2012

[9]   Blamey J., Anthony E.J., Wang J., Fennell P.S. *The calcium looping cycle for large scale CO2 capture*. Progress in Energy and Combustion Science Volume 36, Issue 2

[10]   Markusson N., Shackley S., Eva B. *The social dynamics of carbon capture and storage.* Routledge. 2012.

[11]   IPPC. *Informe especial del IPPC. La captación y almacenamiento del dióxido de carbono. Resumen para Responsables de Políticas y Resumen Técnico*. ISBN 92-9169-319-7. 2005.

[12]   Gibbin, J., Chalmers, H. *Carbon Capture and Storage*. Energy Policy. Volume 36, Issue 12, December 2008, pp. 4317-4322.

[13]   IPCC. Working Group III. *Carbon dioxide capture and storage: Special report of the IPCC.*

[14]   Richter H.J. and Knoche K.F. (1983). *Reversibility of combustion processes, in Efficiency and Costing – Second law analysis of processes*. ACS symposium series (235). pp. 71–85

[15]   Lyngfelt A. *Oxygen-Carriers for Chemical-Looping Combustion – Operational Experience.* 1st International Conference on Chemical Looping. Lyon, 17-19 March 2010.

[16]   Adanez J., Abad A., Garcia-Labiano F., Gayan P., de Diego L.F. *Mapping of the range of operational conditions for Cu-, Fe-, and Ni-based oxygen carriers in chemical-looping combustion.* Chemical Engineering Science. 62 (2007), Issues 1-2, pp. 533-549.

[17] Leion H. *Capture of CO_2 from solid fuels using Chemical-Looping Combustion and Chemical-Looping Oxygen Uncoupling*. Doctoral Thesis. Chalmers University Of Technology. Gothenburg, Sweden. 2008

[18] Mattison T., Lyngfelt A., Leion H. *Chemical-Looping with oxygen uncoupling for combustion of solids fuels.* International Journal of Greenhouse Gas Control. 3 (2009), Issue 1, pp. 11-19

[19] Adanez J., Abad A., Garcia-Labiano F., Gayan P., de Diego L.F. *Demonstration of chemical-looping with oxygen uncoupling (CLOU) process in a 1.5 kWh continuously operating unit using a Cu-based oxygen-carrier*. International Journal of Greenhouse Gas Control. 6 (2012) pp. 189-200.

[20] Jerndal E. *Investigation of Nickel- and Iron-Based oxygen carriers for Chemical-Looping Combustion.* Doctoral Thesis. Chalmers University of Technology. Gothenburg, Sweden. 2010

[21] Johansson M. *Screening of oxygen carrier particles based on iron-, manganese-, copper-, and nickel oxides for use in chemical-looping technologies*. Doctoral Thesis. Chalmers University of Technology. Gothenburg, Sweden. 2007

[22] Kunii D.; Levenspiel O. *Fluidization Engineering*. Ed. Butterworth-Heinemann, 1991.

[23] Reichhold A., Friedl G., Kronberger B. *Temporary Defluidisation in Fine Powder Fluidised Beds Caused By Changing the Fluidization Gas*. Chem.Eng.Technol. 25 (2002) pp. 4

[24] Cho P., Mattisson T., Lyngfelt A. *Defluidization Conditions for a Fluidized Bed of Iron Oxide-, Nickel Oxide-, and Manganese Oxide-Containing Oxygen Carriers for Chemical-Looping Combustion*. Ind. Eng. Chem. Res. 45 (2006) pp. 968-977.

[25] Stobbe E.R.; de Boer B.A.; Geus J.W. *The reduction and oxidation behavior of manganese oxides.* Catalysis Today 47 (1999) pp. 161-167

[26] Azimi G., Rydén M., Leion H., Mattison T. and Lyngfelt A. *$(Mn_zFe_{1-z})_yO_x$ Combined Oxides as Oxygen Carrier for Chemical-Looping with Oxygen Uncoupling*. Alche Journal, 59 (2013), Issue 2, pp. 582-588.

[27] Shulman A., Clevertam E, Mattisson T., Lyngfelt A. *Manganese/Iron, Manganese/Nickel, and Manganese/Silicon Oxides Used in Chemical-Looping With Oxygen Uncoupling (CLOU) for Combustion of CH_4.* Energy Fuels 2009, 33, pp. 5269-5275.

[28] Shulman A., Clevertam E, Mattisson T., Lyngfelt A. *Chemical Looping with oxygen uncoupling using Mn/Mg-based oxygen carriers.*Fuel, 90 (2011) pp. 941-950.

[29] Muan A., *Phase equilibria in the system manganese oxide-SiO_2 in air*, American Journal of Science, 257(1959), pp. 297-315

[30]   Rydén M., Leion H., Mattisson T., Lyngfelt A. *Combined oxides as oxygen-carrier material for chemical-loopingwith oxygen uncoupling.* Applied Energy,113 (2014), pp. 1924-1932.

[31]   Jing D., Mattisson T., Leion H., Rydén M. and Lyngfelt A., *Examination of Perovskite Structure CaMnO$_{3-\delta}$ with MgO Addition as Oxygen Carrier for Chemical Looping with Oxygen Uncoupling Using CH$_4$ and Syngas,* International Journal of Chemical Engineering, Article ID 679560, 16 pages, 2013